Supporting Information

Retracing the Rapid Evolution of an Herbicide-Degrading Enzyme by Protein Engineering

Markus R. Busch[1], Lukas Drexler[1], Dhani Ram Mahato[2], Caroline Hiefinger[1], Sílvia Osuna[2,3], Reinhard Sterner[1*]*

[1]Institute of Biophysics and Physical Biochemistry, Regensburg Center for Biochemistry, University of Regensburg, D-93040 Regensburg, Germany.
[2]CompBioLab Group, Institut de Química Computacional i Catàlisi (IQCC) and Departament de Química, Universitat de Girona, Girona 17003, Spain.
[3]ICREA, Barcelona 08010, Spain.

***Corresponding Authors:**

Sílvia Osuna: Email: silvia.osuna@udg.edu
Reinhard Sterner: Email: reinhard.sterner@ur.de

SUPPLEMENTAL FIGURES

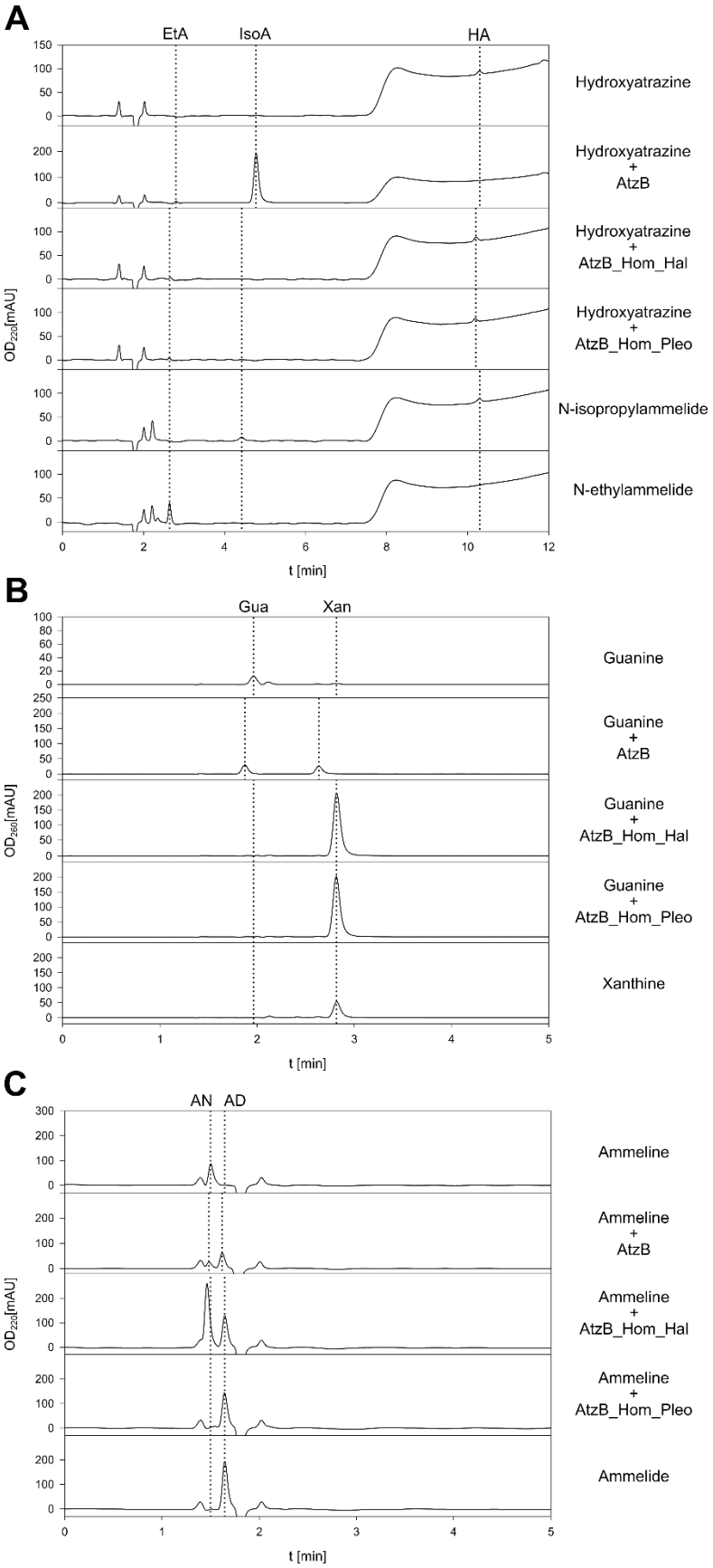

Figure S1: Substrate screening of AtzB, AtzB_Hom_Hal, and AtzB_Hom_Pleo. (A) AtzB specifically turns over hydroxyatrazine (HA) into N-isopropylammelide (IsoA) with only a minor peak of N-ethylammelide (EtA). AtzB_Hom_Hal and AtzB_Hom_Pleo exhibit a weak hydroxyatrazine hydrolase activity, producing mainly EtA. **(B)** Guanine (Gua) is hydrolyzed into xanthine (Xan) by AtzB, AtzB_Hom_Hal, and AtzB_Hom_Pleo. **(C)** All three enzymes exhibit a hydrolytic activity on the anthropogenic substance ammeline (AN), deaminating it to ammelide (AD). Due to column aging, peaks are off-set in some experiments. All enzymatic assays contained 500 μM of the respective substrate and 10 μM of the enzyme variant, which were incubated for 20 h at RT.

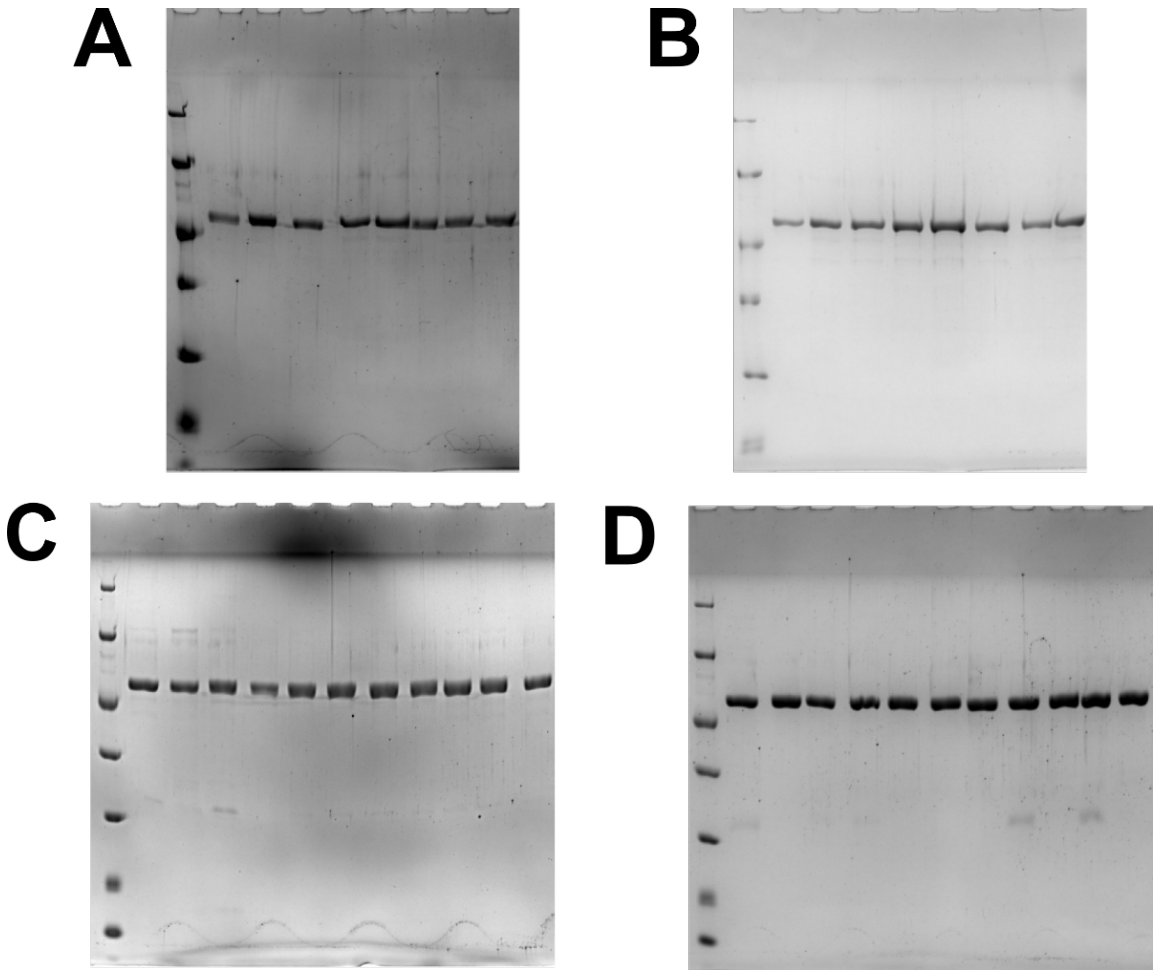

Figure S2: Assessment of protein purity by SDS-PAGE. (A) Bands correspond to protein standard (LMW, Thermo Fisher Scientific), wild-type AtzB, and AtzB variants I170N, S218C, S219Q, I222N, S218C I170N, S218C S219Q, and S218C I222N. **(B)** Bands correspond to protein standard and AtzB variants S219Q I170N, I170N I222N, S219Q I222N, S218C S219Q I170N, S218C S219Q I222N, S218C I170N I222N, S219Q I170N I222N, and S218C S219Q I222N I170N. **(C)** Bands correspond to protein standard, wild-type AtzB_Hom_Hal, and AtzB_Hom_Hal variants N161I, C209S, Q210S, N213I, Q210S N161I, Q210S C209S, Q210S N213I, Q210S N213I C209S, Q210S N213I N161I, and Q210S N213I N161I C209S. **(D)** Bands correspond to protein standard, wild-type AtzB_Hom_Pleo, and AtzB_Hom_Pleo variants N165I, C213S, Q214S, N217I, N217I N165I, N217I C213S, N217I Q214S, N217I N165I C213S, N217I N165I Q214S, and N217I N165I Q214S C213S. Each protein band contains 3 µg of the respective protein variant.

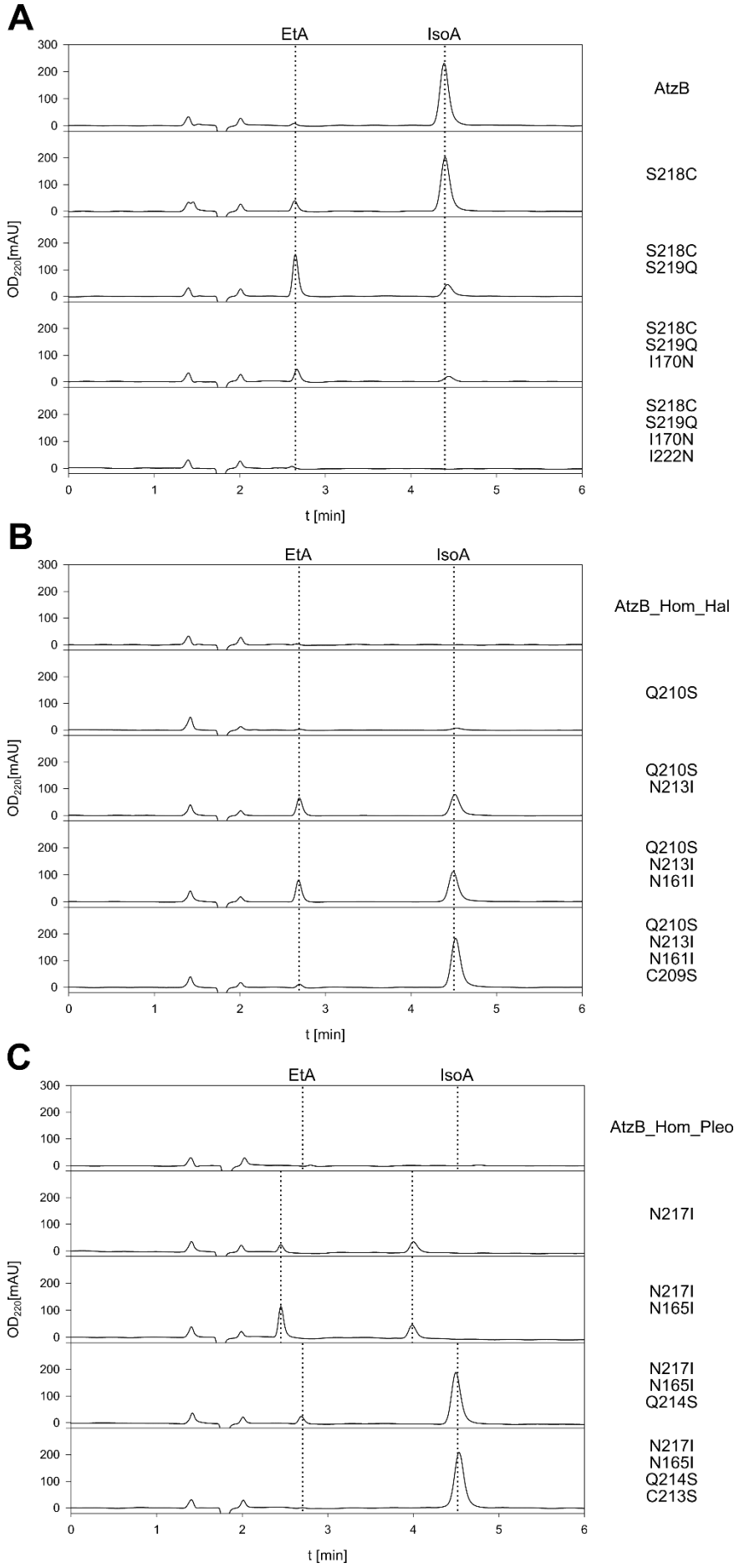
A
EtA
IsoA
AtzB
S218C
S218C
S219Q
S218C
S219Q
I170N
S218C
S219Q
I170N
I222N
OD220[mAU]
t [min]
B
EtA
IsoA
AtzB_Hom_Hal
Q210S
Q210S
N213I
Q210S
N213I
N161I
Q210S
N213I
N161I
C209S
OD220[mAU]
t [min]
C
EtA
IsoA
AtzB_Hom_Pleo
N217I
N217I
N165I
N217I
N165I
Q214S
N217I
N165I
Q214S
C213S
OD220[mAU]
t [min]

Figure S3: Analysis of product mixtures of hydroxyatrazine hydrolysis. Hydroxyatrazine hydrolysis can result in either N-isopropylammelide (IsoA) or N-ethylammelide (EtA). Variants of AtzB **(A)** along the main evolutionary trajectory progressively lose the specificity for hydroxyatrazine ethylaminohydrolysis found in the wild type. Variants of AtzB_Hom_Hal **(B)** and AtzB_Hom_Pleo **(C)** gain selectivity for ethylaminohydrolysis along their respective evolutionary trajectories with the selectivity of the resulting quadruple variants being comparable to that of wild-type AtzB. All reaction mixtures result from the conversion of 500 µM hydroxyatrazine by 2 µM of the respective enzyme over 20 h at 25°C. The results shown here correspond to the ones visualized in Figure 5 in the main text.

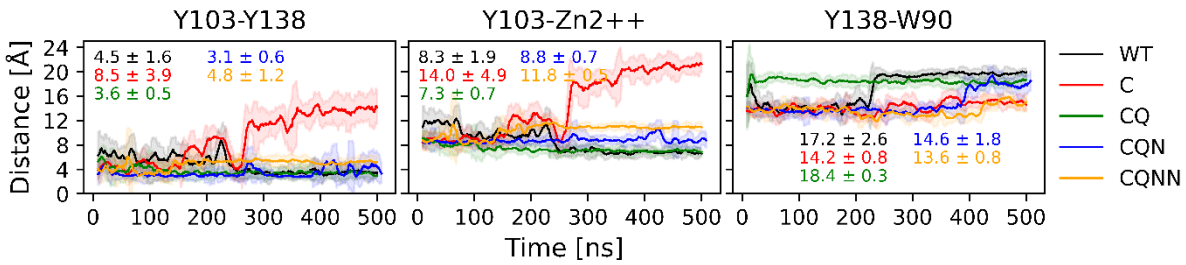

Figure S4. Plot of key active site distances for AtzB, AtzB-C, AtzB-CQ, AtzB-CQN, AtzB-CQNN. Distances (in Angstrom) for the AtzB apo structures: AtzB (black line), AtzB-C (red), AtzB-CQ (green), AtzB-CQN (blue), AtzB-CQNN (yellow). The left plot monitors the distance between the hydroxyl oxygens of Y103(OH) and Y138(OH), the middle plot the distance between the hydroxyl oxygen of Y103(OH) and the Zn(II) atom, and the right plot the distance for the Y138(OH) and the NH of the indole ring of W90.

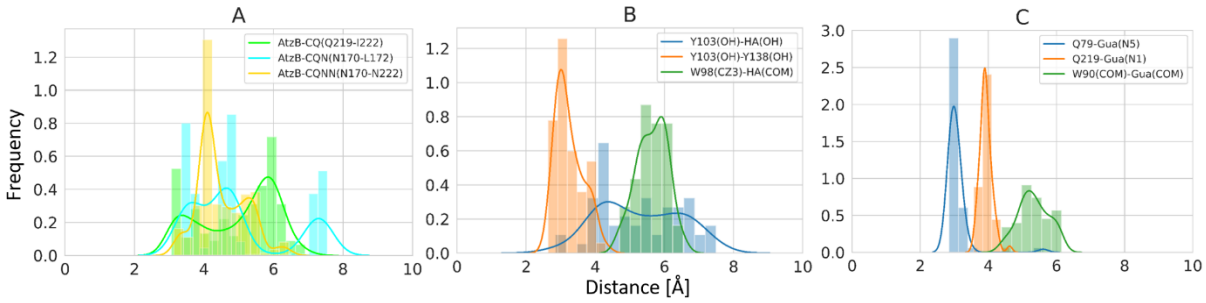

Figure S5. Histogram and distribution plot of key active site distances in (A) apo structures, and AtzB liganded with (B) hydroxyatrazine (HA) and (C) guanine (Gua). All distances are represented in Å.

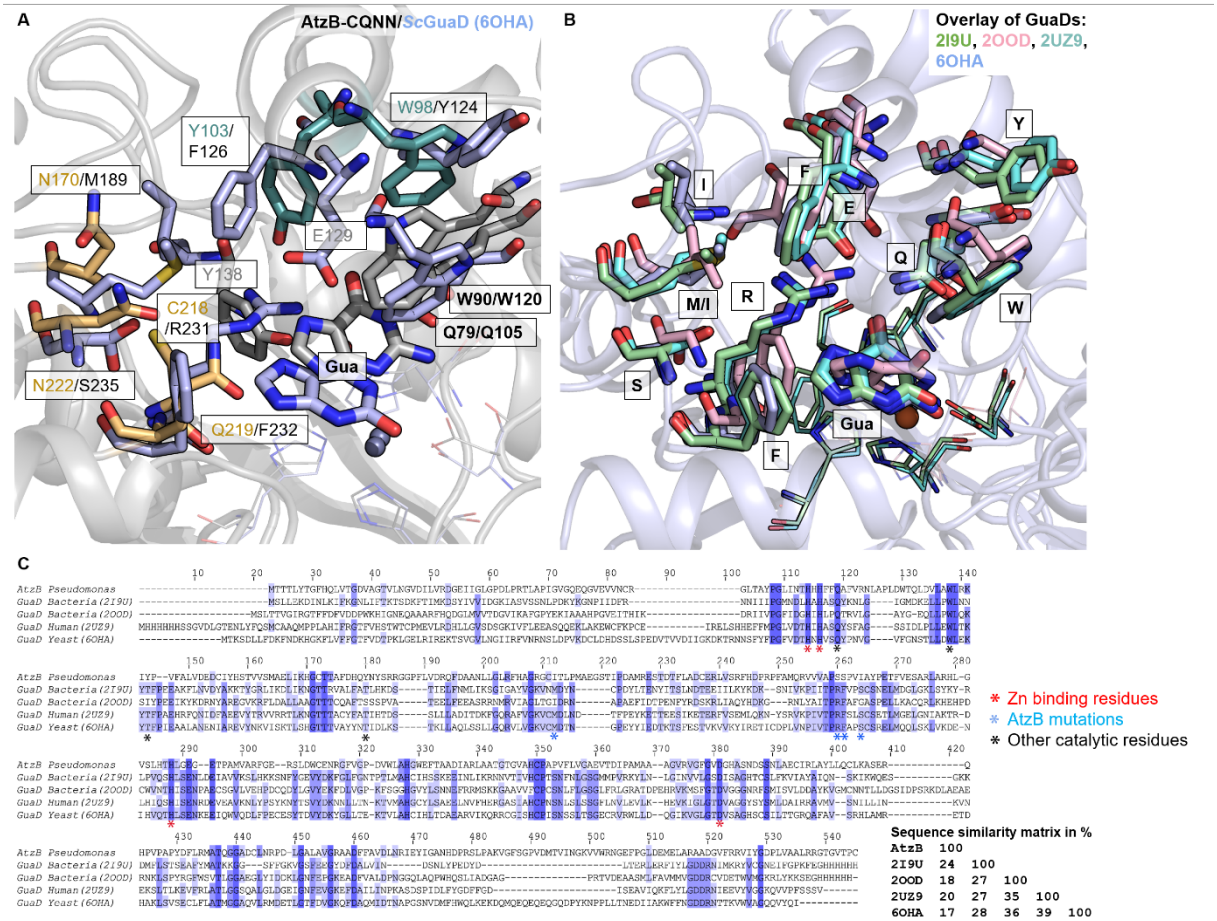

Figure S6. Structural and sequence comparison of liganded guanine deaminases (GuaD) and a representative conformation of AtzB-CQNN with guanine bound from 100 ns MD simulation. (**A**) Overlay of AtzB-CQNN (residues shown in gray, yellow and teal, guanine in gray) with *Saccharomyces cerevisiae* GuaD (PDB code: 6OHA, shown in light blue). (**B**) Overlay of available guanine/xanthine-bound crystal structures of GuaD: 2I9U (*Clostridium acetobutylicum*, green), 2OOD (*Bradyrhizobium diazoefficien*s, pink), 2UZ9 (*Homo sapiens*, cyan) and 6OHA (*Saccharomyces cerevisiae*, light blue). (**C**) Sequence alignment showing the metal binding residues and active site residues. The sequence identity of the GuaD enzymes with respect to AtzB is: 2I9U (24%), 2OOD (18%), 2UZ9 (20%), and 6OHA (17%). Despite having low sequence similarities, GuaDs and AtzB share many of the key active residues for catalysis.

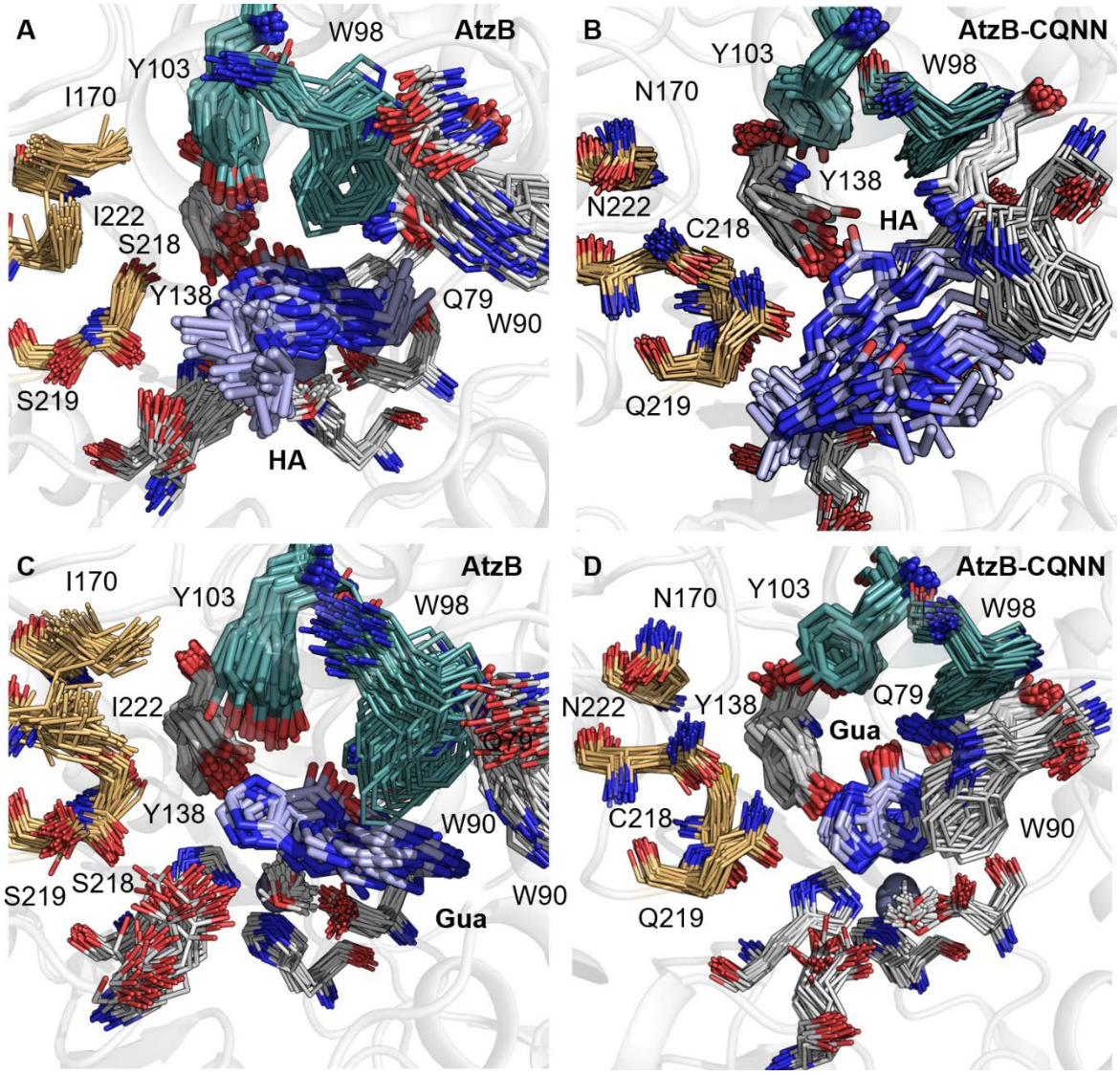

Figure S7. Overlay of conformations explored in the 100 ns MD simulations with either hydroxyatrazine (HA) or guanine (Gua) bound in the AtzB and AtzB-CQNN active sites. The active site of wild-type AtzB bound with different conformations of HA in a productive conformation (**A**), while in AtzB-CQNN structure HA can no longer orient this substrate correctly for catalysis (**B**). Inversely, AtzB cannot productively bind Gua with proper confirmation (**C**), while in AtzB-CQNN (**D**) Gua is correctly positioned.

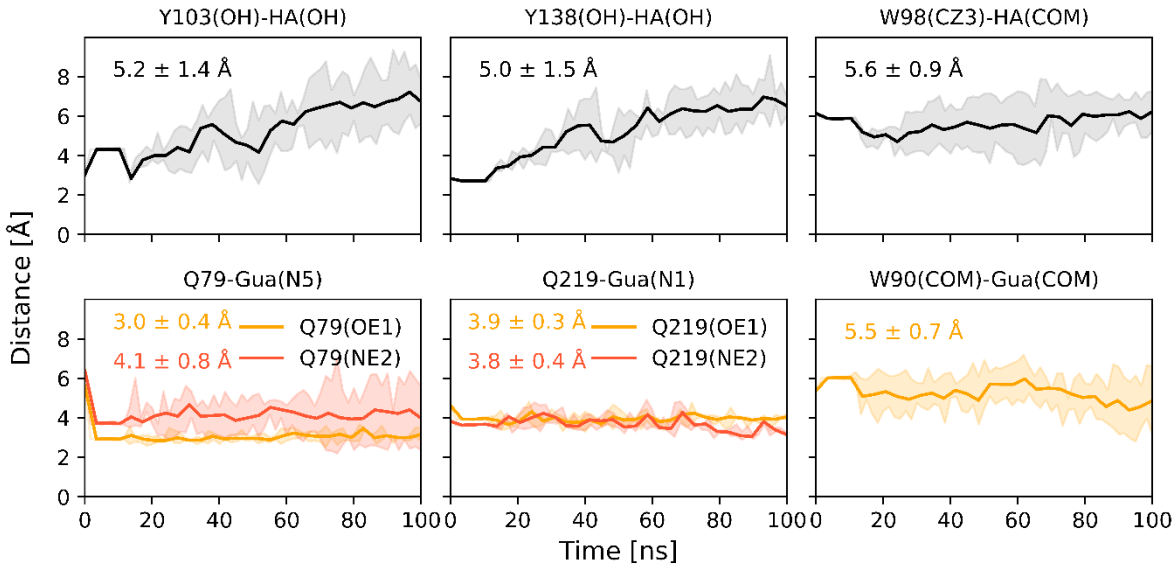

Figure S8. Plot of key active site distances for AtzB, and AtzB-CQNN in the presence of either hydroxyatrazine (HA) or guanine (Gua). Distances (in Angstrom) for AtzB (black line), and AtzB-CQNN (yellow/red).

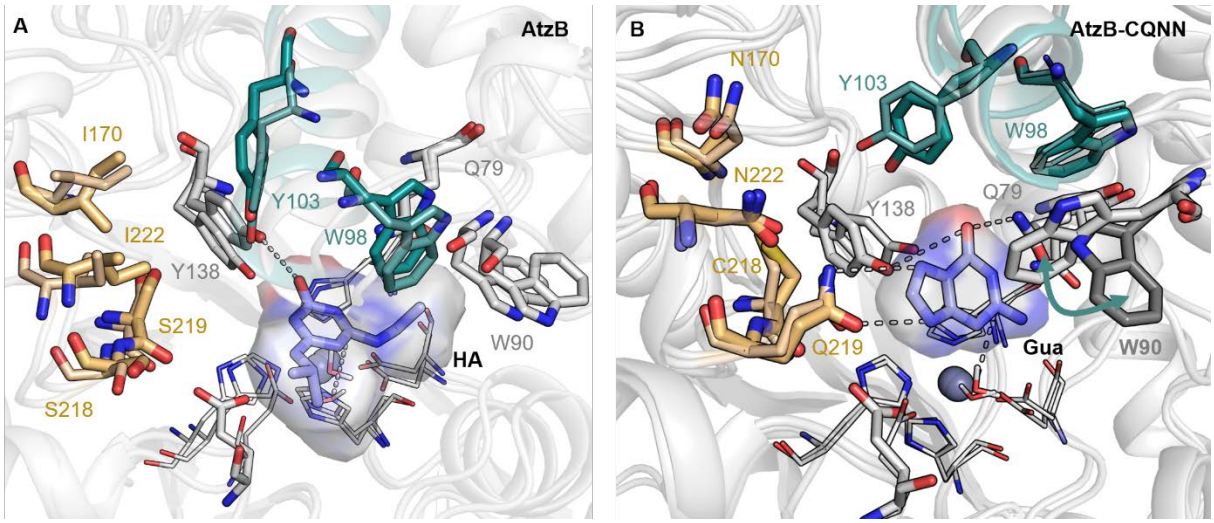

Figure S9. **Overlay of the most populated representative conformation of (A) AtzB and (B) AtzB-CQNN in the unliganded and liganded states.** The conformation of the active site residues is very similar in both cases, the only exception being W90 in AtzB-CQNN. In that case, W90 slightly changes the conformation of the indole ring to maximize and establish a CH $\cdot\cdot\pi$ interaction with guanine.

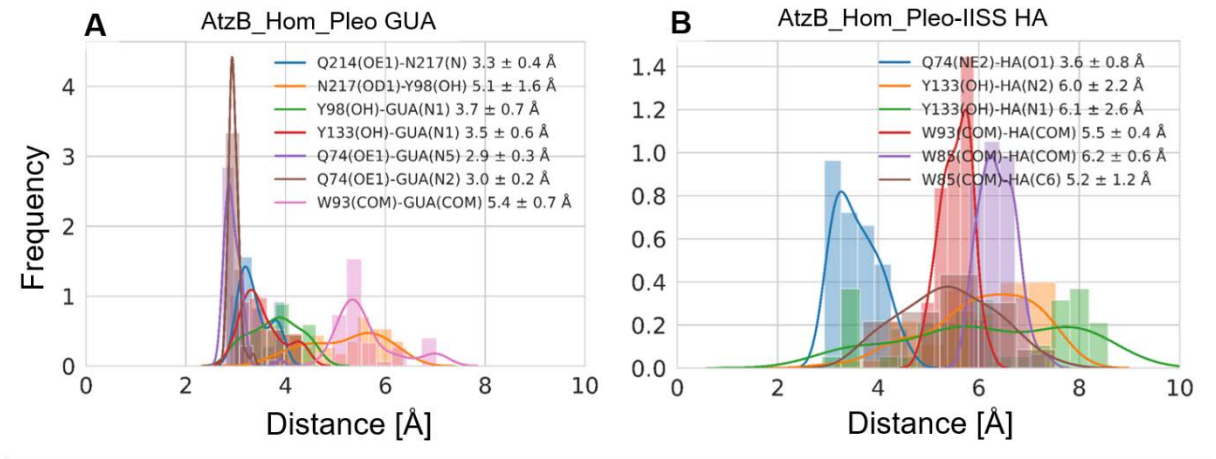

Figure S10: Distance distribution plots for AtzB_Hom_Pleo bound with guanine and hydroxyatrazine substrates. **(A)** Distance (in Å) distribution plots for AtzB_Hom_Pleo with guanine bound. Guanine is in close contact with Q74, Y98 and Y133. **(B)** Distance (in Å) distribution plots for AtzB_Hom_Pleo-IISS with HA bound shows that two residues Q74 and Y133 are in close contact with HA. The distances for W93 and W85 are computed from the center of mass (COM) of the indole and substrate rings.

SUPPLEMENTAL TABLES

Table S1. AtzB proteins and AtzB homologues used to construct sequence logos. The local sequence identity results from a BLAST search with *Pseudomonas sp. strain* ADP AtzB as query protein.

Accession	NCBI-annotation	Organism	Sequence identity
AtzB			
AAC45138.1	MULTISPECIES: amidohydrolase	*Proteobacteria*	100 %
WP_130110726.1	amidohydrolase	*Leucobacter triazinivorans*	98.74 %
ACI14308.1	hydroxyatrazine hydrolase, partial	*Pseudomonas sp.* AD39	99.22 %
WP_192321895.1	amidohydrolase family protein	*Aminobacter sp.* SR38	99.38 %
BAD69556.1	hydroxyatrazine hydrolase	*beta proteobacterium* CDB21	99.37 %
AAY40323.2	hydroxysimazine hydrolase[+]	*Herbaspirillum sp.* B601	99.58 %
WP_011777000.1	MULTISPECIES: amidohydrolase	*Micrococcaceae*	100 %
ERI35184.1	amidohydrolase	*Arthrobacter sp.* AK-YN10	99.79 %
AGU71906.1	hydroxyatrazine hydrolase	*Arthrobacter sp.* DNS10	99.79 %
ACC78169.1	hydroxyatrazine hydrolase, partial	*Arthrobacter sp.* AD26	100 %
AtzB Homologues			
WP_135441588.1	amidohydrolase family protein	*Haliea sp.* SAOS-164	65.38 %
WP_026793093.1	amidohydrolase	*Pleomorphomonas oryzae*	61.47 %
WP_101287147.1	amidohydrolase	*Pleomorphomonas diazotrophica*	60.56 %
NTJ65121.1	amidohydrolase	*Agrobacterium rhizogenes*	59.58 %
OHC53060.1	amidohydrolase	*Rhodobacterales bacterium*	59.54 %
WP_132536943.1	amidohydrolase	*Rhizobium sp.* PP-F2F-G48	59.48 %
WP_062694026.1	amidohydrolase	*Rhizobium sp.* Leaf341	59.35 %
WP_062472743.1	MULTISPECIES: amidohydrolase	unclassified *Rhizobium*	59.35 %
WP_183711985.1	MULTISPECIES: amidohydrolase	unclassified *Rhizobium*	59.35 %
MBO9628520.1	amidohydrolase	*Shinella sp.*	59.35 %
WP_251730559.1	amidohydrolase family protein	*Pleomorphomonas sp.* NRK KF1	59.28 %
WP_095436959.1	amidohydrolase	*Rhizobium sp.* 11515TR	59.11 %
MBS1168142.1	hydroxydechloroatrazine ethylaminohydrolase (hydroxyatrazine hydrolase)[++]	*Proteobacteria bacterium*	58.93 %

WP_054007318.1	amidohydrolase	*Cypionkella psychrotolerans*	58.92 %
WP_183872653.1	amidohydrolase	*Rhizobium sp*. BK491	58.88 %
WP_092852053.1	amidohydrolase	*Rhizobium miluonense*	58.88 %
WP_069614677.1	MULTISPECIES: amidohydrolase	unclassified *Rhizobium*	58.88 %
WP_015342298.1	MULTISPECIES: amidohydrolase	*Rhizobium*	58.88 %
WP_075632883.1	amidohydrolase	*Rhizobium rhizosphaerae*	58.86 %
WP_120669701.1	MULTISPECIES: amidohydrolase	unclassified *Rhizobium*	58.72 %
WP_145646153.1	MULTISPECIES: amidohydrolase	unclassified *Rhizobium*	58.64 %
WP_112343490.1	amidohydrolase	*Rhizobium tropici*	58.64 %
WP_149633722.1	amidohydrolase	*Rhizobium tropici*	58.64 %
WP_104827655.1	MULTISPECIES: amidohydrolase	*Rhizobium*	58.64 %
WP_081177750.1	amidohydrolase	*Rhizobium rhizosphaerae*	58.41 %
OYU38210.1	MAG: amidohydrolase	*Pseudorhodobacter sp*. PARRP1	58.24 %
SIQ86939.1	hydroxyatrazine ethylaminohydrolase	*Rhizobium sp*. RU35A	58.17 %
WP_149747129.1	amidohydrolase	*Rhizobium sp*. RU35A	58.17 %
WP_146366487.1	amidohydrolase	*Qingshengfaniella alkalisoli*	58.13 %
WP_252733080.1	amidohydrolase family protein	*Shimia thalassica*	58.12 %
WP_183799496.1	amidohydrolase	*Rhizobium sp*. BK316	58.07 %
WP_062368869.1	amidohydrolase	*Rhizobium altiplani*	58.01 %
WP_139075739.1	amidohydrolase	*Rubellimicrobium rubrum*	58.00 %
WP_092584509.1	amidohydrolase	*Rhizobium mongolense*	58.00 %
WP_215570083.1	amidohydrolase	*Rhizobium sp*. CSW-27	57.94 %
WP_127906158.1	amidohydrolase	*Mesobaculum littorinae*	57.92 %
WP_007825584.1	amidohydrolase	*Rhizobium sp*. CF142	57.88 %
WP_074065066.1	MULTISPECIES: amidohydrolase	*Rhizobium*	57.88 %
WP_216759008.1	amidohydrolase	*Rhizobium sp*. WYJ-E13	57.88 %
WP_210529277.1	MULTISPECIES: amidohydrolase	unclassified *Rubellimicrobium*	57.81 %

[+] Categorized as AtzB protein due to extremely high sequence identity with the query protein.

[++]Categorized as AtzB homologue due to limited sequence identity with the query protein and lack of experimental characterization.

Table S2. Catalytic parameters of mutants of AtzB, AtzB_Hom_Hal, and AtzB_Hom_Pleo for the deamination of guanine.

Protein	k_{cat} [s^{-1}]	K_M [µM]	k_{cat}/K_M [$M^{-1}s^{-1}$]
AtzB	-	-	n.d. [a]
I170N	-	-	n.d. [a]
S218C	-	-	9.8±0.23 [b]
S219Q	-	-	n.d. [a]
I222N	-	-	n.d. [a]
S218C I170N	-	-	13±0.66 [b]
S218C S219Q	-	-	43±1.3 [b]
S218C I222N	-	-	2.9±0.10 [b]
S219Q I170N	-	-	n.d. [a]
I170N I222N	-	-	7.0±0.34 [b]
S219Q I222N	4.4e-3 ± 3.6e-4	93±20	47±14
S218C S219Q I170N	-	-	61±2.3 [b]
S218C S219Q I222N	-	-	n.d. [a]
S218C I170N I222N	-	-	2.5e2±8.3 [b]
S219Q I170N I222N	-	-	45±1.3 [b]
S218C S219Q I222N I170N	0.21±8.0e-3	53±6.6	3.9e3±6.4e2
AtzB_Hom_Hal	0.062±2.1e-3	56±6.1	1.1e3±1.6e2
N161I	-	-	n.d. [a]
C209S	0.028±0.010	7.4e2±3.5e2	38±32
Q210S	0.095±0.012	6.5e2±1.1e2	1.4e2±44
N213I	-	-	54±0.64 [b]
Q210S N161I	-	-	n.d. [a]
Q210S C209S	-	-	n.d. [a]
Q210S N213I	-	-	13±0.21 [b]
Q210S N213I C209S	-	-	n.d. [a]
Q210S N213I N161I	-	-	n.d. [a]
Q210S N213I N161I C209S	-	-	n.d. [a]
AtzB_Hom_Pleo	0.15±2.7e-3	67±3.6	2.2e3±1.6e2
N165I	0.026±4.7e-3	3.1e2±1.0e2	84±42
C213S	8.5e-3±1.2e-3	5.3e2±1.1e2	16±5.6
Q214S	0.017±2.7e-3	5.6e2±1.3e2	30±12
N217I	0.036±0.010	4.3e2±1.8e2	85±59
N217I N165I	0.090±0.025	9.0e2±3.1e2	1.0e2±62
N217I C213S	-	-	n.d. [a]
N217I Q214S	0.032±3.3e-3	8.4e2±1.1e2	38±8.9
N217I N165I C213S	-	-	n.d. [a]
N217I N165I Q214S	-	-	n.d. [a]
N217I N165I Q214S C213S	-	-	n.d. [a]

Mean values and standard deviations are derived from triplicate measurements. [a] n.d.: no detectable activity in the presence of 10 µM enzyme and 300 µM substrate; [b] Values were determined from the linear dependence of the enzyme turnover rate on substrate concentration.

Table S3. Catalytic parameters of mutants of AtzB, AtzB_Hom_Hal, and AtzB_Hom_Pleo for the hydrolysis of hydroxyatrazine.

Protein	k_{cat} [s^{-1}]	K_M [µM]	k_{cat}/K_M [$M^{-1}s^{-1}$]
AtzB	5.3±0.66	21±7.8	2.4e5±1.2e5
I170N	2.1±0.12	52±5.7	4.1e4±6.9e3
S218C	2.1±0.13	41±5.3	5.2e4±1.0e4
S219Q	1.7±0.13	44±6.9	3.8e4±9.1e3
I222N	0.35±0.018	35±3.9	1.0e4±1.6e3
S218C I170N	1.9±0.20	1.3e2±19	1.5e4±3.7e3
S218C S219Q	0.60±0.081	34±11	1.8e4±8.1e3
S218C I222N	0.43±0.035	60±8.7	7.1e3±1.6e3
S219Q I170N	0.086±4.1e-3	65±5.4	1.3e3±1.7e2
I170N I222N	0.062±2.2e-3	9.3±1.3	6.7e3±1.2e3
S219Q I222N	0.030±1.7e-3	48±5.2	6.3e2±1.0e2
S218C S219Q I170N	0.13±0.012	27±6.4	4.8e3±1.6e3
S218C S219Q I222N	0.33±0.021	45±5.7	7.4e3±1.4e3
S218C I170N I222N	0.078±2.3e-3	18±1.5	4.4e3±5.2e2
S219Q I170N I222N [a]	-	-	11 [b]
S218C S219Q I170N I222N	7.9e-3±2.6e-4	27±2.2	2.9e2±33
AtzB_Hom_Hal	-	-	n.d. [c]
N161I	-	-	n.d. [c]
C209S	-	-	n.d. [c]
Q210S	7.7e-3±4.0e-4	16±2.6	4.8e2±1.0e2
N213I	0.025±3.4e-3	71±16	3.5e2±1.3e2
Q210S N161I	0.010±8.3e-4	43±7.3	2.3e2±59
Q210S C209S	4.4e-3±2.0e-4	9.9±1.4	4.4e2±81
Q210S N213I	0.051±1.8e-3	42±3.0	1.2e3±1.3e2
Q210S N213I C209S	0.052±2.4e-3	23±2.8	2.2e3±3.6e2
Q210S N213I N161I	0.068±2.2e-3	20±1.8	3.4e3±4.1e2
Q210S N213I N161I C209S	0.44±0.026	19±3.1	2.3e4±5.1e3
AtzB_Hom_Pleo	4.9e-3±6.7e-4	1.2e2±23	42±14
N165I	0.029±7.9e-3	1.3e2±50	2.3e2±1.5e2
C213S	1.0e-3±9.3e-5	15±4.3	69±27
Q214S	0.020±1.1e-3	28±3.9	7.0e2±1.4e2
N217I	0.075±5.0e-3	77±9.3	9.8e2±1.8e2
N217I N165I	0.15±9.8e-3	23±3.9	6.7e3±1.6e3
N217I C213S	0.11±0.022	1.1e2±34	9.5e2±4.9e2
N217I Q214S	0.46±0.072	89±22	5.1e3±2.1e3
N217I N165I C213S	1.5±0.13	70±11	2.1e4±5.2e3
N217I N165I Q214S	1.1±0.050	19±2.3	5.9e4±9.8e3
N217I N165I Q214S C213S	7.5±0.29	28±2.6	2.7e5±3.5e4

Mean values and standard deviations are derived from triplicate measurements.[a] Single measurement; [b] Values were determined from the linear dependence of the enzyme turnover rate on substrate concentration.; [c] n.d.: no detectable activity in the presence of 1 µM enzyme and 75 µM substrate.

Table S4. Synthesized genes used in this work.

AtzB	ATGACCACCACACTGTATACCGGTTTTCATCAGCTGGTTACCGGTGATGT TGCAGGCACCGTTCTGAATGGTGTTGATATTCTGGTTCGTGATGGTGAAA TTATTGGTCTGGGTCCTGATCTGCCTCGTACACTGGCACCGATTGGTGTT GGTCAAGAACAGGGTGTTGAAGTTGTTAATTGTCGTGGTCTGACCGCATA TCCGGGTCTGATTAATACCCATCATCATTTTTTTCAGGCCTTTGTGCGTA ATCTGGCACCGCTGGATTGGACCCAGCTGGATGTTCTGGCATGGCTGCGT AAAATCTATCCGGTTTTTGCACTGGTTGATGAGGATTGCATTTATCATAG CACCGTTGTTAGCATGGCCGAACTGATTAAACATGGTTGTACCACCGCAT TTGATCACCAGTATAACTATAGCCGTCGTGGTGGTCCGTTTCTGGTTGAT CGTCAGTTTGATGCAGCAAATCTGCTGGGTCTGCGTTTTCATGCAGGTCG TGGTTGTATTACCCTGCCGATGGCAGAAGGTAGCACCATTCCGGATGCAA TGCGTGAAAGCACCGATACCTTTCTGGCAGATTGTGAACGTCTGGTTAGC CGCTTTCATGATCCGCGTCCGTTTGCAATGCAGCGTGTTGTTGTTGCACC GAGCAGTCCGGTTATTGCCTATCCGGAAACCTTTGTTGAAAGCGCACGTC TGGCACGTCATCTGGGTGTTAGCCTGCATACCCATTTAGGTGAAGGTGAA ACACCGGCAATGGTTGCACGTTTTGGTGAACGTAGCCTGGATTGGTGTGA AAATCGTGGTTTTGTTGGTCCGGATGTTTGGCTGGCACATGGTTGGGAAT TTACCGCAGCAGATATTGCCCGTCTGGCAGCAACCGGCACCGGTGTTGCA CATTGTCCGGCACCTGTTTTTCTGGTGGGTGCAGAAGTTACCGATATTCC TGCAATGGCAGCAGCCGGTGTTCGTGTTGGTTTTGGCGTTGATGGTCATG CAAGCAATGATAGCAGCAATCTGGCAGAATGTATTCGTCTGGCATACCTG CTGCAGTGTCTGAAAGCAAGCGAACGTCAGCATCCGGTTCCGGCACCGTA TGATTTTCTGCGTATGGCAACCCAAGGTGGTGCAGATTGTCTGAATCGTC CGGATCTGGGTGCACTGGCAGTTGGTCGTGCAGCCGATTTTTTTGCAGTG GATCTGAATCGCATTGAATATATTGGTGCAAATCATGATCCTCGTAGCCT GCCTGCAAAAGTTGGTTTTAGCGGTCCGGTTGATATGACCGTTATTAATG GTAAAGTTGTGTGGCGCAATGGTGAATTTCCTGGTCTGGATGAAATGGAA CTGGCACGTGCAGCAGATGGTGTTTTTCGTCGTGTTATTTATGGTGATCC GCTGGTTGCAGCACTGCGTCGTGGTACAGGTGTTACCCCGTGT
AtzB_Hom_Hal	ATGAGCACCGTTCTGTTTCGTAATTTTCGTCAGCTGGTTTGTGCGGGTGC ACCGGGTAGCGTTCTGCGTGATGTTGATCTGTGTGCACGTGATGGTATGA TTACCGCAATTGGTCCGCAGCTGCCGCTGACCGATGTTGATGAAGTTGTT GATTGTGGTGGTCTGACCGCATATCCTGGTCTGGTTAATACCCATCATCA TTTTTTTCAGGCCCTGGTTCGTAATCTGCCAGGTCTGGATTGGACCACAC TGAGCCTGCTGGAATGGCTGGATACCATTTATCCGATTTTTGCACGTCTG GATGAGGATTGTATTTATCATGCAAGCCTGATTAGCCTGGCCGATCTGCT GAAACATGGTTGTACCACCGCATTTGATCACCAGTATAACTTTAATAGCA ATATGGGTAGCCGTGTTGTGGATCGTCAGTTTGAAGCAGCAGCACTGCTG GGTGCCCGTCTGCATGTTGGTCGTGGTTGTAATACCCTGCCGATGAGCGC AGGTAGCACCATTCCGGATGCAATGCTGGAAACCACCGATGCATTTCTGG CCGATTGTGAACGTCTGATTGGTGCATTTCATAATCCGGCACCGGGTGCA ATGGCACAGGTTGTTGTTGCACCGTGTCAGCCGGTTAATAGCCTGCCGGA AACCTTTCCGGAAGCCGCAGCGCTGGCACGTCGTCATGGTGTTCGTCTGC ATACCCATCTGAGCGAAGGTGAAAATGCAGCCATGCTGGATCGTTTTGGT ATGCGTAGCCTGGATTGGTGTGAAAGCGTTGGTTTTGTTGGTCCGGATGT TTGGTTTGCACATGGTTGGGAATTTACCCCTCCGGAAATTGCGCGTCTGG CAGCAACCGGTACAGGTGTTGCACATTGTCCGGCTCCGGTTTTTCTGGTT GGTGCAGAAGTTACCGATCTGCCTGCAATGGTTGCAGCAGATATGACCGT TGGTATGGGTGTTGATGGTCAGGCAAGCAATGATAGCAGCAATCTGGCAG AATGTATGCGTCTGGCCTACCTGCTGCAGTGTCTGAATGCACGCCATAAT CCGCTGCCTGCACCGCCTCCGGAACGTTATCTGCATATGGCAACCGCAGG CGGTGCCGCATGTCTGGGTCGTACCGATATTGGTGAACTGGCAGTTGGTA AAGCAGCAGATTTTTTCTGTGCAGATCTGAATGGCCTGGATTATGCCGGT GCAGATAGCGATCCGCTGAGTCTGCCTGCCAAAGTGGGTTTTGCAGGTCC

	GGCAGCAATGACCGTGGTTCATGGTCGTGTTGTTTGGCGTGATGGTGAAT TTCCGGGTTTAGATGAAACCCAGCTGCGTAGCGCAGCAGATGCCCTGCTG CGTGAAAAACTGGATGGTCATCTGGCACCGCTGCGTACACCGGGT
AtzB_Hom_Pleo	ATGGGCAACTATCTGCTGAAAAATTGTGCAGCAGTTATGGTTGATGATGG TGCAGGTCTGAATGCACGTCGTAATGTTGATATTCTGACCGATGGTCCGG CAATTAAAGCAATTGAACCGCATCTGGCAGAAACACCGCAGAGCGTTGGT GCCGAAGTTATTGATGCAAGCGGTTGGTTTGTTTATCCTGGTCTGGTTAA TACCCACCACCATTTTTTTCAGACCTTTGTTCGTAATCGTGCAGAACTGG ATTGGACCAAACTGAGCGTTCTGGAATGGCTGGATCGTATTTATCCGATT TTTAGCCAGCTGACCGAAGATTGCTTTTATCATAGCAGCCTGACCGCAAT GGCAGAACTGATTAAACATGGTTGTACCACCGCACTGGATCATCAGTATT GTTTTCCGCGTCATGCAGGTAAATATCTGGTTGATCGTCAGTTTGAAGCA GCAGAACGTCTGGGTATTCGTTATCATGCCGGTCGTGGTGGTAATACCCT GCCGAAAAGCGAAGGTAGCACCATTCCGGATGCAATGCTGGAAACCACCG ATGAATTTCTGGCAGATTGTGAACGTCTGATTGATCGCTATCATGATGCA AGTCCGTTTAGCCTGCGTCAGGTTGTTATTAGCCCGTGTCAGCCGGTTAA TAGCTATCGTGAAACCTTTGTTGAAAGCGTTGCACTGGCACGTGATAAAG GTGTTTTTCTGCATACCCATGTTGGTGAAGGTGAAAGTCCGGTTATGGAA GCACGTCATGGTAAACGTACCGTTGATTATCTGGAAGAAATGGGTTTTGC AGGTCCGGATGTTTTTTATGCACATTGTTGGGAACTGACCCATACCGAAC TGGCAAAACTGGCAGCAAGCGGCACCGGTGTTAGCCATTGTCCGGAACCG GTTTATCTGGTGGGTGCAGAAGTTACCGATATTCCAGCCATGGCAGCACT GGGTGTTCGTGTTGGTCTGGGTTGTGATGGTAGCGCAAGCAATGATAATA GTAATCTGATGCATTGCATTCATAGCGCCTATATGCTGCAGTGTCTGGTT GCAAGCAGCCGTAGCCATCCTGTTCCGGCACCGGCAGAATTTCTGCGTTT TGCAACCACCGGTAGCGCCAGCCTGCTGGGTCGTGCAGATATTGGTCGTC TGGCACCTGGTATGGCAGCAGACCTGTTTGCAATTGATACCCGTCGTATG GATTATGTTGGCACCCGTCATGATCCGCTGAGCCTGCCTGCAAAATTAGG TATTGGTATGGCCACCGATCTGACCATGATTAATGGTCGTATTGTTTGGG CCAATGGTGAATTTCCGGGTATTGATGAAGCAGAAATGGCAGCCGAAGCA GAAGCAACCCTGGCAACCATTGATTTT

Table S5. Nucleotide primers used in this work.

Name	Sequence	Use
CyRI	TCACGAGGCCCTTTCGTCTT	Forward sequencing primer (pUR22)
CyPstI	TCGCCAAGCTAGCTTGGATTCT	Reverse sequencing primer (pUR22)
EcAtzB_pET21a_fw	AAAAAAGGTCTCACATGACCACCACACTGTATACCGG	Cloning of codon optimized *atzB* gene
EcAtzB_pET21a_rv	TTTTTTGGTCTCTCGAGACACGGGGTAACACCTGTACC	Cloning of codon optimized *atzB* gene
EcGuaD_fw_pET21a _BsaI	AAAAAAGGTCTCACATGATGTCAGGAGAACAC	Cloning of wild-type *guaD* gene (*E. coli*)
EcGuaD_rv_pET21a _BsaI	TTTTTTGGTCTCTCGAGGTTGCGTTCGTACAC	Cloning of wild-type *guaD* gene (*E. coli*)
EcAtzB-Hom-Hal _fw_pET21a_BsaI	AAAAAAGGTCTCACATGAGCACCGTTCTGTTTCG	Cloning of codon optimized *atzB_Hom_Hal* gene
EcAtzB-Hom-Hal _rv_pET21a_BsaI	TTTTTTGGTCTCTCGAGGCCCGGTGTACGCAGC	Cloning of codon optimized *atzB_Hom_Hal* gene
EcAtzB-Hom-Pleo _fw_pET21a_BsaI	AAAAAAGGTCTCACATGGGCAACTATCTGCTG	Cloning of codon optimized *atzB_Hom_Pleo* gene
EcAtzB-Hom-Pleo _rv_pET21a_BsaI	TTTTTTGGTCTCTCGAGAAAATCAATGGTTGCCAGGG	Cloning of codon optimized *atzB_Hom_Pleo* gene
AtzB_N139C_fw	TGCTATAGCCGTCGTGGTGG	Mutagenesis (with AtzB_N139C_rv)
AtzB_N139C_rv	ATACTGGTGATCAAATGCGGTGG	Mutagenesis
AtzB_I170N_fw	AACACCCTGCCGATGGCAG	Mutagenesis (with AtzB_I170N_rv)
AtzB_I170N_rv	ACAACCACGACCTGCATGAAAACG	Mutagenesis
AtzB_S218C_fw	TGCAGTCCGGTTATTGCCTATCCGG	Mutagenesis (with AtzB_S218 S219_rv)
AtzB_S219Q_fw	AGCCAGCCGGTTATTGCCTATCCGG	Mutagenesis (with AtzB_S218 S219_rv)
AtzB_S218C_S219Q_fw	TGCCAGCCGGTTATTGCCTATCCGG	Mutagenesis (with AtzB_S218 S219_rv)
AtzB_S218-S219_rv	CGGTGCAACAACAACACGCTGCATTGCAAACGGAC	Mutagenesis
AtzB_I222N_fw	AACGCCTATCCGGAAACCTTTGTTGAAAGC	Mutagenesis (with AtzB_I222_A223_rv; AtzB_C_I222_A223_rv; AtzB_CQ_I222_A223_rv)
AtzB_A223S_fw	ATTAGCTATCCGGAAACCTTTGTTGAAAGCGC	
AtzB_I222N_A223S_fw	AACAGCTATCCGGAAACCTTTGTTGAAAGC	
AtzB_I222_A223_rv	AACCGGACTGCTCGGTGCAAC	Mutagenesis
AtzB_C_I222_A223_rv	AACCGGACTGCACGGTGCAAC	Mutagenesis (maintains S218C background)
AtzB_CQ_I222_A223_rv	AACCGGCTGGCACGGTGCAAC	Mutagenesis (maintains S218C S219Q background)
AtzB_C169G_fw	GGCATTACCCTGCCGATGGC	Mutagenesis (with AtzB_C169G_rv)
AtzB_C169G_I170N_fw	GGCAACACCCTGCCGATGGC	Mutagenesis (with AtzB_C169G_rv)
AtzB_C169G_rv	ACCACGACCTGCATGAAAACGC	Mutagenesis
AtzB_Hom_Hal_N161I_rv	AGGGTAATACAACCACGACCAACATGCAGACGGG	Mutagenesis (with AtzB_Hom_Hal_N161_rv)
AtzB_Hom_Hal_N161_rv	AGGGTATTACAACCACGACCAACATGCAGACGGG	Mutagenesis
AtzB_Hom_Hal_N213I _fw	GTTATTAGCCTGCCGGAAACCTTTCCGGAAGCC	Mutagenesis (with AtzB_Hom_Hal_C209S_Q210Q_rv; AtzB_Hom_Hal_C209C_Q210S_rv; AtzB_Hom_Hal_C209S_Q210S_rv; AtzB_Hom_Hal_C209C_Q210Q_rv)
AtzB_Hom_Hal_N213N _fw	GTTAATAGCCTGCCGGAAACCTTTCCGGAAGCC	
AtzB_Hom_Hal _C209S_Q210Q_rv	CGGCTGGCTCGGTGCAACAACAACCTGTGCC	Mutagenesis
AtzB_Hom_Hal _C209C_Q210S_rv	CGGGCTACACGGTGCAACAACAACCTGTGCC	Mutagenesis

AtzB_Hom_Hal _C209S_Q210S_rv	CGGGCTGCTCGGTGCAACAACAACCTGTGCC	Mutagenesis
AtzB_Hom_Hal _C209C_Q210Q_rv	CGGCTGACACGGTGCAACAACAACCTGTGCC	Mutagenesis
AtzB_Hom_Pleo_N165_fw	CCGAAAAGCGAAGGTAGCACCATTCCGG	Mutagenesis (with AtzB_Hom_Pleo_N165I_rv)
AtzB_Hom_Pleo_N165I_rv	CAGGGTAATACCACCACGACCGGCATGATAACG	Mutagenesis
AtzB_Hom_Pleo_N217I _fw	GTTATTAGCTATCGTGAAACCTTTGTTGAAAGCG	Mutagenesis (with AtzB_Hom_Pleo_C213S_Q214Q_rv; AtzB_Hom_Pleo_C213C_Q214S_rv; AtzB_Hom_Pleo_C213S_Q214S_rv; AtzB_Hom_Pleo_C213C_Q214Q_rv)
AtzB_Hom_Pleo_N217N _fw	GTTAATAGCTATCGTGAAACCTTTGTTGAAAGCG	
AtzB_Hom_Pleo _C213S_Q214Q_rv	CGGCTGGCTCGGGCTAATAACAACC	Mutagenesis
AtzB_Hom_Pleo _C213C_Q214S_rv	CGGGCTACACGGGCTAATAACAACC	Mutagenesis
AtzB_Hom_Pleo _C213S_Q214S_rv	CGGGCTGCTCGGGCTAATAACAACC	Mutagenesis
AtzB_Hom_Pleo _C213C_Q214Q_rv	CGGCTGACACGGGCTAATAACAACC	Mutagenesis
AtzB_Hom_Pleo_N217I _in_Q214S_rv	CGGGCTACACGGGCTAATAAC	Mutagenesis (with AtzB_Hom_Pleo_ N217I_fw)